Electrochimica Acta 55 (2009) 327–339

Contents lists available at ScienceDirect

Electrochimica Acta

journal homepage: www.elsevier.com/locate/electacta

Self-organization phenomena at semiconductor electrodes

H. Föll*, M. Leisner, A. Cojocaru, J. Carstensen

Institute for Materials Science, Christian-Albrechts-University of Kiel, Kaiserstrasse 2, 24143 Kiel, Germany

ARTICLE INFO

Article history:
Received 27 November 2008
Received in revised form 30 March 2009
Accepted 31 March 2009
Available online 7 April 2009

Keywords:
Self-organization
Electrochemistry of semiconductors
Pore formation
Self-induced oscillations
Silicon

ABSTRACT

Anodically dissolving semiconductor electrodes such as Si, Ge, GaAs, InP, or GaP exhibit a number of self-organization phenomena such as current oscillations in time and/or in space; some phenomena of this kind are also found during the anodic formation of porous metal oxides. Current oscillations in space are expressed in correlated pore growth and other effects like pore diameter oscillation; this will be introduced and discussed in some detail. Some less well-known effects like self-induced growth mode transitions or pore density oscillations are also included. The paper endeavors to sort through the various self-organization phenomena observed so far and to look for underlying principles that transcend semiconductor-specific dissolution chemistry. Intrinsic time and length scales provide one such principle and this will be discussed with emphasis on the so-called current burst model originally developed for current oscillations in time.

1. Introduction

During the electrochemical anodic dissolution of single crystals of semiconductors such as Si, Ge, and III–V's, a number of self-organization processes is observed. Most prominent in this respect are the self-induced current oscillations of p-type Si electrodes at relatively high potentials around 5 V in aqueous HF electrolytes, cf. for example [1–5] and the references therein. The word "oscillation" in this context refers to some periodic behavior of a relevant quantity in time and is seen as an expression of some self-organization; oscillations in time have also been found during galvanostatic (i.e. constant current) experiments for the voltage in Si (cf. [6]), more recently a number of papers also addresses voltage or current oscillations in InP [7–10]. Self-induced oscillations in time of the open-circuit potential in Si were observed, too [11]; and many more observations of this general topic have been reported and will be addressed to some extent in what follows.

Fig. 1 gives some illustrative examples different from the usually observed rather stable current oscillations at HF concentrations of a few wt%, cf., e.g. [1–5,12]. Shown are damped current oscillations (Fig. 1a) and stable voltage oscillations (Fig. 1b). While the question has been raised if sustained oscillations, i.e. oscillations with no damping at all and thus always relying on some intrinsic synchronization mechanism, do exist in this context (the Palaiseau group around Chazalviel and Ozanam recently denied this [13]), here we simply consider damped oscillations, including heavily damped ones as shown in Fig. 1a, to be still an expression of some self-organization. These oscillations clearly express an intrinsic time constant of the system in the ms or s range that is far larger than any time constants that can be associated with the concomitant chemical reactions on an atomic scale.

Less well known are oscillations of the current in space as exemplified in Fig. 2a. The self-organized pore crystal in InP shown in this example (after [14]) formed because at the place of a pore (dark region) the localized current flow has dissolved InP (to a depth of >300 μm), while in between the pores the current density was zero or at least very small. The current distribution on the sample surface thus is periodic in two dimensions; the resulting single pore crystal (with defects) must be interpreted as the result of a self-organized current oscillation in space. Fig. 2b and c, which will be discussed in more detail in what follows, show pore arrangements that can be interpreted as damped current oscillations in space. Even Fig. 2d, where the pore and thus the current distribution shows no directly obvious periodicity, is not completely random with respect to pore sizes and pore distances. These current oscillations in space clearly express an intrinsic length scale of the system typically in the 50 nm to 5 μm range that is far larger than length scales that can be associated with the lengths scales of chemical reactions on an atomic scale, or even with the typical thicknesses of intermediate product layers like SiO_2.

There are more expressions of self-organization than current oscillations in time and space that can be found during the anodic dissolution of semiconductors, and this paper makes a first attempt at a systematic review of what has been found so far, including some rather new findings in Si. For the sake of brevity and readability the large topic of how to form pores in semiconductors will not be discussed, nor will all experimental details around the examples shown be reproduced. The reader is referred to the literature cited,

* Corresponding author. Tel.: +49 431 880 6176; fax: +49 431 880 6178.
E-mail address: hf@tf.uni-kiel.de (H. Föll).

0013-4686/$ – see front matter © 2009 Elsevier Ltd. All rights reserved.
doi:10.1016/j.electacta.2009.03.076

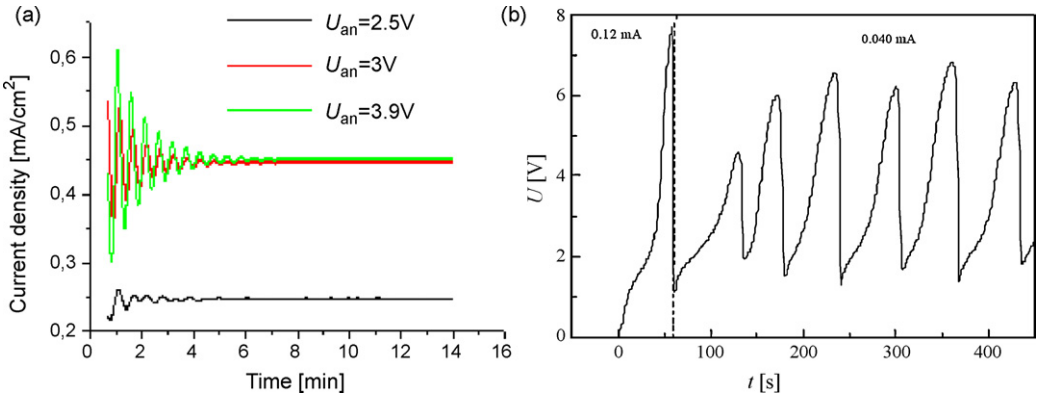

Fig. 1. Examples of oscillations in time found with Si electrode at very low HF concentrations around 0.1 wt%. (a) Damped current oscillations at potentiostatic conditions. (b) Voltage oscillations at galvanostatic conditions. Initiating these oscillations needs a "nucleation" period at 0.12 mA as shown.

and to the following overview articles and reviews in the literature [1,15–23].

To what extent the various instances of self-organization rely on comparable basic mechanisms is an open question at present. While oscillations in time for Si have been extensively studied and several models have been proposed, not much modeling has been done with respect to oscillations in space, or other self-organization effects. The paper will attempt to highlight some of the possible mechanisms discussed at present, but cannot present mature theories because they do not yet exist. It is very likely, however, that some general mechanism can be found that will be able to account for many expressions of self-organization in various semiconductors from common general principles.

2. Oscillations in time and the current burst model

Current oscillations obtained during anodic dissolution were noted about 150 years ago by Faraday [24] and are rather common in electrochemistry. Oscillations were found in such systems as, e.g. Ni and Fe electrodes in H_2SO_4 solution [25–29], Cu in HCl [30–32], iron in chloride solutions [33], to name just a few. Several theoretical models were formulated that tried to explain oscillating electrodes and chemical oscillations in general already many years ago [34–36] and many papers appeared with respect to the particularly well pronounced current (and voltage) oscillations in Si; here we give only references to the newest papers of the major groups working in this field. Besides the Kiel group of the authors, advocating the so-called "current burst model" (CBM), see [6,37,38] and the references therein, the Berlin group around Lewerenz and Grzanna has been very active in this field, promoting a model based on Markov chains; see [4,39,40] and the references therein. Both groups provide a "microscopic" point of view, looking at basic processes at the Si electrode. The Munich group around Krischer and the Palaiseau group around Chazalviel and Ozanam take a different "top down" approach, looking at the non-linear differential equations describing the system, cf. [3,12,41–44] and the references therein. To what

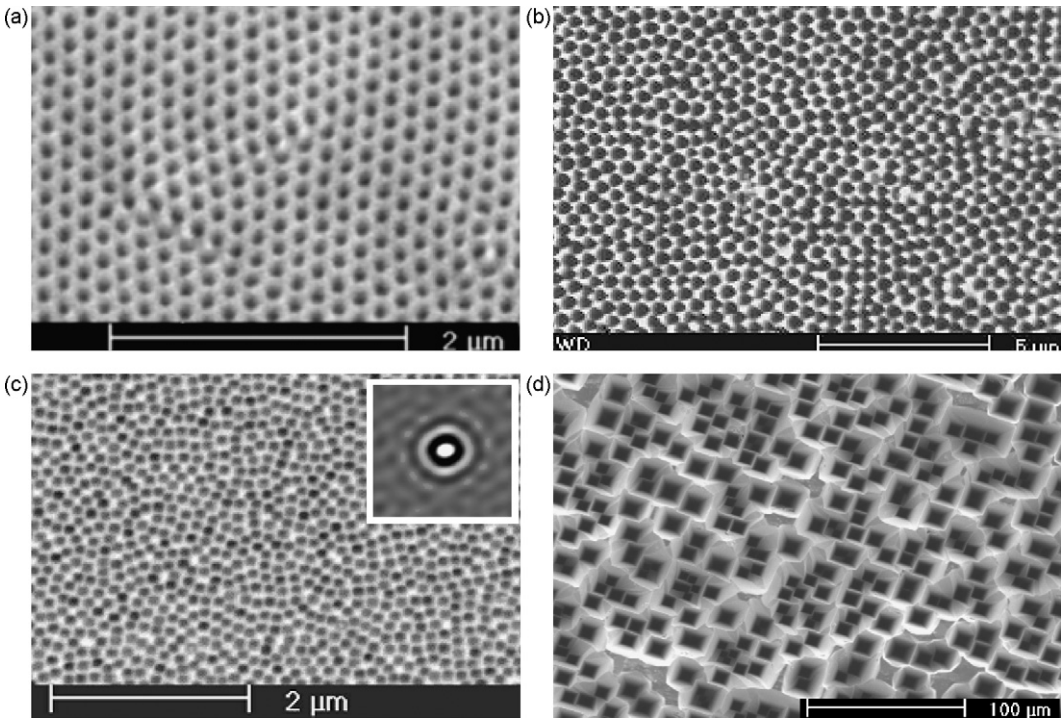

Fig. 2. Examples of current oscillations in space. (a) Single pore crystal in {1 0 0} n-type InP. (b) Short range order ("damped oscillation") in {1 1 1} n-type Si. (c) Frustrated crystal (see text for details) in {1 0 0} n-type Si. (d) Random pore distribution in {1 0 0} n-type Ge obtained in an HCl electrolyte (note the much larger scale).

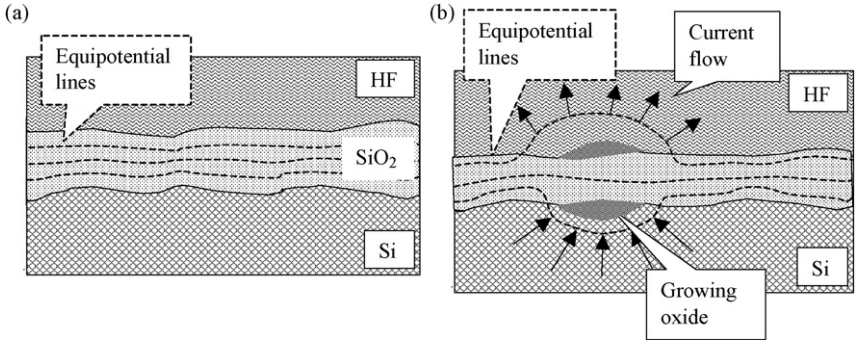

Fig. 3. Essentials of the current burst model. (a) Thick oxide with some roughness, no current flow yet. The voltage drops almost completely in the oxide with equipotential lines as shown. (b) Oxide has dissolved somewhat; the field strength at some point is large enough to initiate local breakdown and a current burst. Local oxide growth produces an "oxide bump"; the electrical field and current flow adjust as schematically indicated.

extent these models can be carried over to well-developed voltage oscillations observed by now quite frequently in InP during pore etching or otherwise [7–10] or Ge [23] remains to be seen.

In what follows we will briefly introduce and discuss the current burst model, because it is the most advanced model in terms of quantification and comparison with oscillation-in-time experiments. The current burst model can also easily be generalized in a qualitative way. The CBM, for example, is the only model at present that can simulate voltage oscillations in Si with good accuracy relative to experiments. While quite different from the other models

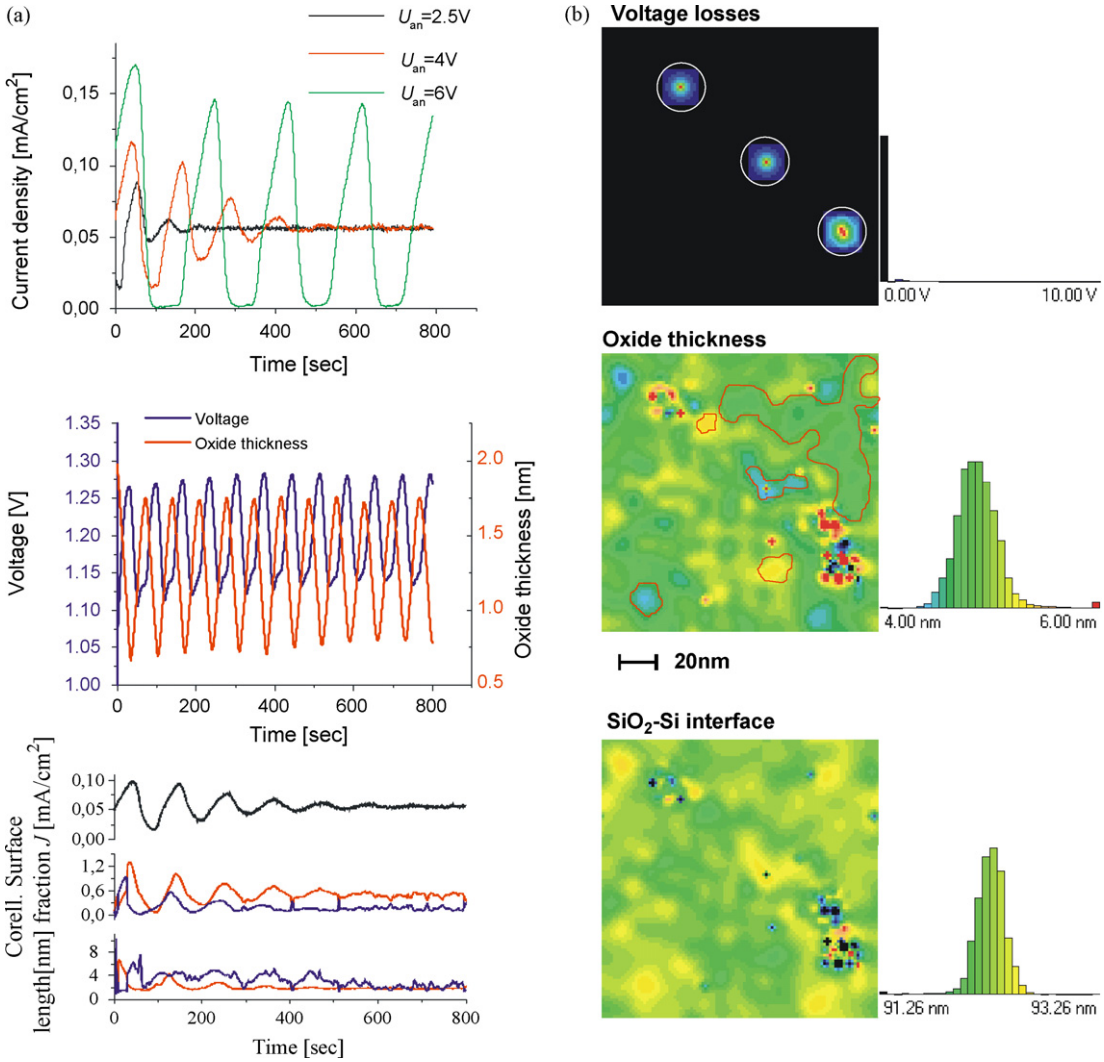

Fig. 4. Examples of results for oscillations in time obtained from Monte Carlo simulations based on the CBM. (a) Some calculated curves. Top to bottom: examples for damping of current oscillations as a function of the potential. Voltage oscillations and average oxide thickness; note the phase shift. Current, domain size, and correlation length for damped oscillation (red: growing domain; black: shrinking domain). (b) Some calculated maps of (top to bottom): local voltage losses (indicating freshly nucleated current bursts here), oxide thickness, Si–SiO_2 interface roughness. The color scale is always quantitative as indicated by the histograms. (For interpretation of the references to color in this figure legend, the reader is referred to the web version of the article.)

mentioned above, it is not necessarily incompatible (at least to some extent) with the other models mentioned (in fact, Grzanna et al. from the Berlin group have recently incorporated "current bursts" in their model [45]). The CBM, however, is presently limited to small areas and small current densities (and thus thin oxide layers) and therefore cannot deal with, e.g. stresses in the oxide, or the formation of "large" (>100 nm) phase–coupled domains on the sample surface or, to be more general, pattern formation during oscillatory electrode reactions; a topic in the focus of the Munich group.

The CBM model is conceptually simple. Its basic assumption is that current flow through a semiconductor electrode often proceeds over a local barrier and that this barrier is typically overcome in a non-linear fashion. The concept becomes clear by looking at the electropolishing of Si, i.e. a dissolution reaction occurring by the electrochemical formation of oxide followed by purely chemical oxide dissolution. In this case the Si electrode is covered with a thin (several nm) layer of oxide at all times during electropolishing.

If, for ease of conception, we start potentiostatically with a relatively thick SiO_2 layer as shown in Fig. 3a, there will be no current flow at all for some constant potential. The applied voltage will completely drop in the SiO_2 with equipotential lines as shown. In an HF bearing electrolyte the SiO_2 will slowly dissolve and the field strength inside the oxide thus increases. For a typical voltage of 5 V and a thickness of 5 nm, the nominal field strength is 10 MV/cm and this is around the known breakdown field strength of good SiO_2. Electrical breakdown will then undoubtedly occur at some critical field strength, inducing current flow at a still finite oxide thickness.

The only critical assumption of the CBM is: breakdown will not happen globally but locally in small nanometer sized regions with a probability depending on the local field strength. Local breakdown induces a local "current burst" (CB) that generates some oxide locally, resulting in an "oxide bump" (Fig. 3b). Owing to the finite conductivity of electrolyte and Si, the equipotential lines and current flow lines redistribute as shown schematically in Fig. 3b. The growing "oxide bump" decreases the field strength locally and current flow will stop with some probability, again depending on the field strength, after some (average) charge ΔC has been passed. The "switching-off" field strength will generally be lower than the "switching-on" field strength; there will be some hysteresis like in all known kinds of field-triggered electrical discharge phenomena.

After a CB stops, the oxide dissolves again, the field strength goes up, and a new CB is eventually initiated after some average time Δt_{CB}.

This is all. Note that the probabilities defined above introduce a stochastic component into the CBM. Pattern formation in time, i.e. current (or voltage) oscillations, is now possible because there is an intrinsic microscopic current-on–current-off stochastic "oscillator", as defined by the CB cycle. Note also that the current I flows no longer continuously with a magnitude given by $I = Q/t$ (Q = charge passed continuously in space and time with t) but is just an average (in time and space) over the individual $I = \Delta Q/\Delta t_{CB}$ contributions, with ΔQ = charge passed in a CB during its total duration Δt_{CB}. The CBM thus intrinsically contains a time constant Δt_{CB} that is tied to SiO_2 dissolution kinetics and can be rather large. Macroscopic pattern formation (i.e. current oscillations in time) is now possible if the microscopic oscillators synchronize to an appreciable amount. Synchronization of intrinsically random events is generally needed if large-scale order in time and/or space is to emerge out of stochastic small-scale processes and finding a suitable synchronization process is often the difficult part in this kind of approach (cf., e.g. the alternative model for current oscillations of the Berlin group [4,39,40]).

In this respect it is a particular strength of the CBM that it does not need a specific synchronization mechanism since the model already contains one. Synchronization "automatically" happens as soon as the oxide bumps are close enough to interact, i.e. as soon as some percolation limit is reached at higher current densities = higher CB density in space. If some CB happens to nucleate between "older" oxide bumps, it does not have to grow as much oxide as an isolated CB to turn itself off again. This implies that its cycle time is now correlated to some extent to that of its neighbors. In other words: an interaction of current bursts via their products

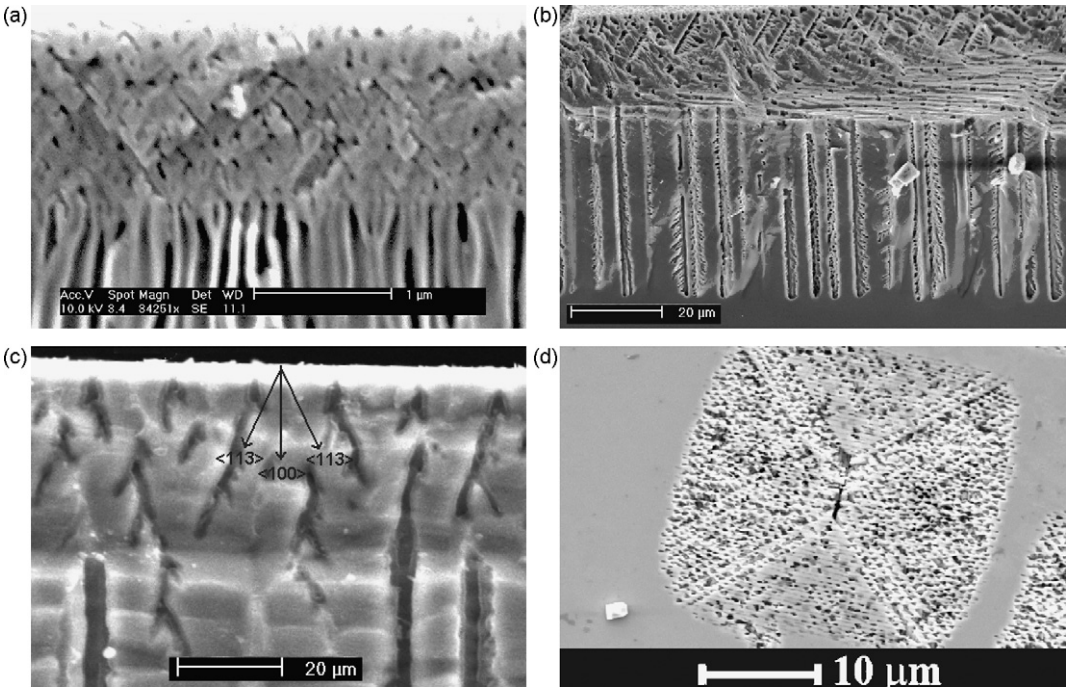

Fig. 5. Growth mode transitions and pore ordering in space. (a) Branching crysto pores in {1 0 0} n-type InP with a self-induced growth mode transition to curro pores that will show some ordering (pore crystal formation). (b) Similar phenomenon in n-type {1 1 1} Si. (c) New finding in {1 0 0} n-type Si showing a growth mode transition reminiscent of the {1 0 0} InP case. (d) Pore domain in GaAs generated by repeated branching started by one central pore.

in space leads to a correlation of CBs in time. As it turns out in a quantitative analysis, this model-inherent synchronization mechanism is already sufficient to synchronize CBs and to model the current/voltage oscillations in the electropolishing region quantitatively in great detail [6].

Fig. 4 gives an example of what the CBM, implemented into a Monte Carlo routine, can deliver. Within the limits discussed above, the CBM is by far the simplest yet most powerful model for current and voltage oscillations at present.

The CBM has not yet been applied to pore formation in Si in a quantitative way. It has been shown qualitatively, however, that it can in principle account for some features of pore formation [46] and it will be evoked a few times in what follows.

3. Pore crystals and ordered pore domains

Fig. 2a shows the most spectacular instance of a pore crystal; an extensive study for this case was presented in [14]. Other high-quality examples of the self-induced formation of pore crystals can be found in porous Al_2O_3 [47], TiO_2 [48], and ZrO_2 [49]. The InP case as shown here has the remarkable feature that a close-packed hexagonal lattice forms on a {1 0 0} oriented substrate; i.e. the underlying symmetries are not compatible. Langa et al. [14,22] have shown that this can be understood by considering the pore nucleation in detail. In the case shown, the pore crystal only forms with so-called "current line" or "curro" pores for short, that grow in the direction of current flow, i.e. more or less perpendicular to the surface. These curro pores cannot form directly but are always preceded by pores oriented into some crystallographic direction (⟨1 0 0⟩ or ⟨1 1 3⟩ for Si [50], and ⟨1 1 1B⟩ for III–V's [14,22]); the cross-sections given in Fig. 5 illustrate this. The initially randomly nucleated crysto pores in Fig. 5a–c branch repeatedly in the downwards and upwards direction (see also Section 6), producing a pore distribution in some depth of the sample with not only a higher pore density than on the surface, but also with some ordering along ⟨1 1 0⟩ directions. Fig. 5d shows this effect rather strikingly for GaAs in a top-view picture. The domains of pores visible at the sample surface with some ordering in just one direction are a result of repeated branching (up and down) of just one central pore and its offspring; the intersection of the pores growing upwards form the domain pattern shown. For details consult [22,51]. Depending on the etching conditions, at some depth a self-induced growth mode transition from crysto to curro pores takes place with the curro pores now forming a more or less well developed single crystal. We use the example to introduce and define qualitatively the term "growth mode transition" (for more details cf. [52]) and to point out that growth mode transitions (self-induced or triggered by changing some external parameter beyond a critical value) of the kind shown must be counted among the "self-organization" features discussed in this paper.

Of course, there must be some interaction between the pores if a regular array or a current oscillation in space is to result; this interaction occurs at the latest as soon as the space charge regions around the pores start to overlap.

Frey et al. [50] tried to emulate the conditions necessary for curro pores and pore crystal formation as they could be deduced from the InP results (large current densities and little oxidation) with Si with some success. Fig. 5b shows a transition from ⟨1 0 0⟩ crysto pores in {1 1 1} n-type Si to curro pores, Fig. 2b and c some arrangements of the resulting curro pores on cuts perpendicular to the pores. While Fig. 2b indicates that some interaction tries to induce close packing on the {1 1 1} oriented samples (there is clearly some short-range hexagonal order), Fig. 2c shows the result for {1 0 0} Si, which seems to indicate a perfectly random structure. That is, however, not the case: what has been formed is a so-called "frustrated crystal", a pore arrangement that tries to be hexagonal (attempt at close packing) and square (attempt to follow the substrate symmetry) as much as possible at the same time. This is clearly demonstrated by the inset, which shows the angular correlation function. While the probability for finding a next neighbor to a given pore is the same for any angle or direction, the probability for second-nearest neighbors has well-developed maxima at 12 specific directions, indicating that there is some order in this arrangement. We will encounter frustrated structures again, and while "frustration" of this sort is well known for, e.g. magnetic moments in crystals [53,54] or for some liquid crystal phases [55], the frustrated structures shown here are

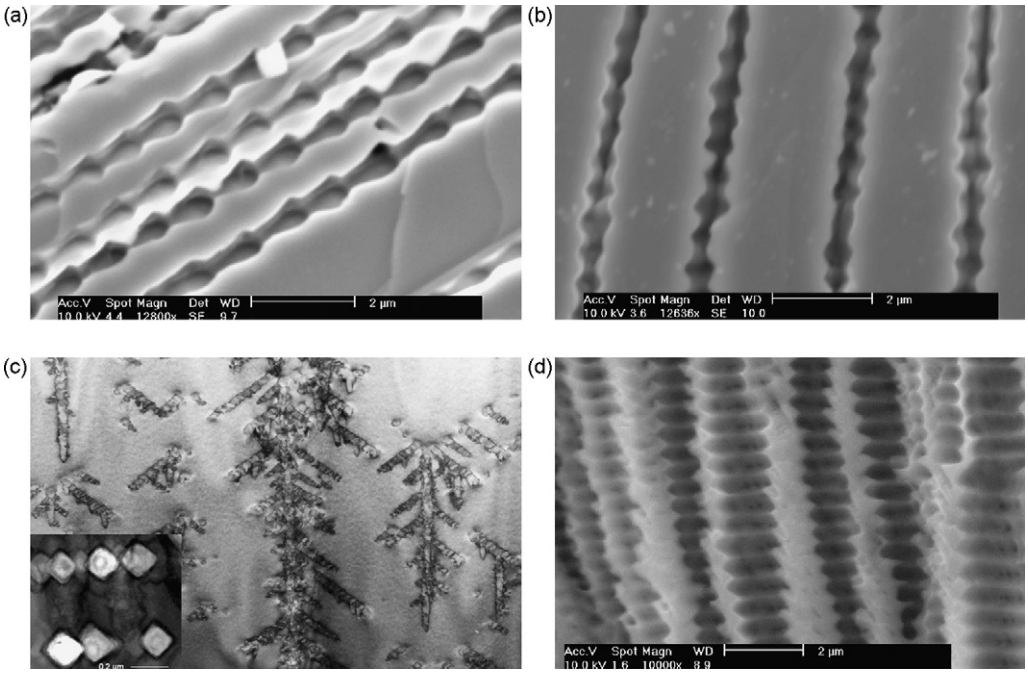

Fig. 6. Self-induced pore diameter oscillations. (a) Crysto pores in GaAs. (b) Curro pores in InP. (c) Crysto pores in Si (TEM picture; insert shows details). (d) Curro pores in n-type Si.

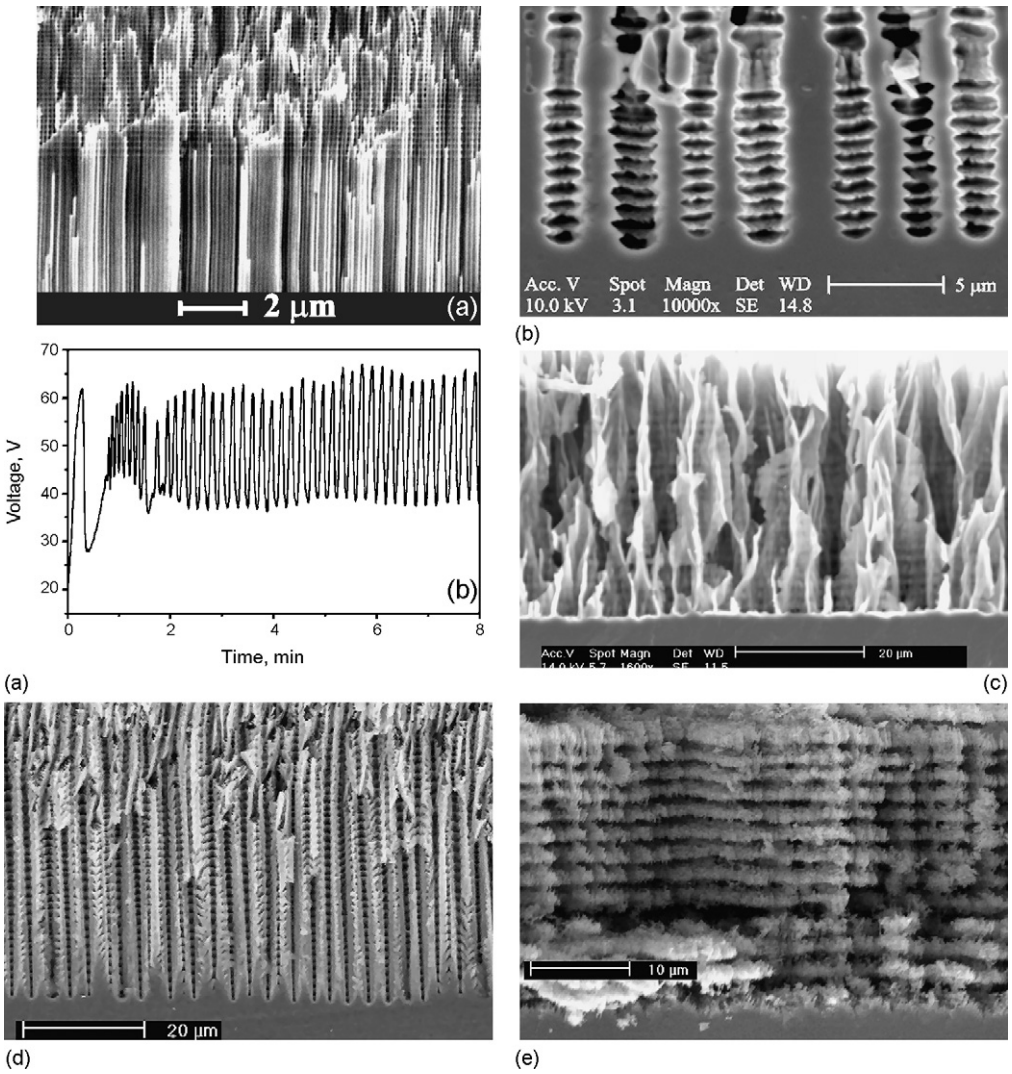

Fig. 7. Correlated pore diameter oscillations. (a) Curro pores in InP with self-induced pore diameter oscillations in the upper half, accompanied by strong voltage oscillations. (b) Curro pores in InP with self-induced pore diameter oscillations in the final stage of pore growth. (c) Curro pores in GaP with self-induced pore diameter oscillations visible as faint horizontal lines. (d) Curro pores in Si with pseudo-oscillations (see text for details). (e) Curro pores in Si with strong correlated pore diameter oscillations bordering on periodic cavity formation producing a "layer cake" structure.

probably the first instances where frustration can be directly seen on a macroscopic length scale.

4. Pore diameter and pore direction oscillations

Self-induced pore diameter oscillations have been observed in several instances. They occur without any correlation between neighboring pores (i.e. random phases) and with strong correlations of at least two kinds. Fig. 6 shows some examples of uncorrelated or at best weekly correlated diameter oscillations in three different semiconductors.

There are different kinds of diameter modulations. First, we have pore growth with strong crystallographic confinements that proceeds by clearing out {1 1 1} bounded tetrahedral (Fig. 6a and b) or octahedral cavities (Fig. 6c) [56] with a size corresponding to the pore geometry that are then staggered like pearls on a chain. This is a process that can be understood to some extent by invoking the CBM together with $\{h\,k\,l\}$ dependent passivation kinetics of freshly etched surfaces [57]. Note that the CBM in this case occurs on two levels: the nanoscopic current bursts described in Section 2 combine in time and space to produce the big meta-CB that obviously clears out an octahedron or tetrahedron, as the case might be. Fig. 6d shows some different behavior that on the one hand might still fit into the octahedral chain model but on the other hand might be a pre-cursor for the correlated pore diameter oscillations shown in Fig. 7. Second, we may encounter rather small diameter variations, then often with strong correlations between the pores. Third, there might be also pseudo-oscillations, like the ones shown in Fig. 7d. In this case of curro pores in {1 1 1} n-type Si, the pore actually tries to follow crystallographic directions and branches periodically in the three accessible ⟨1 1 3⟩ directions, but is forced back into the current line directions by the interaction with its neighbors. The pore in this case does not consist of staggered tetrahedra but of staggered "tripods".

Fig. 7a merits a closer look. The cross-section shown belongs to a well-formed single pore crystal from the type shown in Fig. 1a; the in-phase pore diameter oscillations shown turn it into a self-organized pore crystal in three-dimensions. Whenever this kind of three-dimensional oscillation of the pore geometry in space is observed under galvanostatic conditions, the voltage invariably will oscillate strongly, too. This is easily understood, if one assumes that the current flowing through a single pore generally will show self-induced oscillations (a natural feature of the CBM, but not yet discussed in any other model). As long as there is no phase cou-

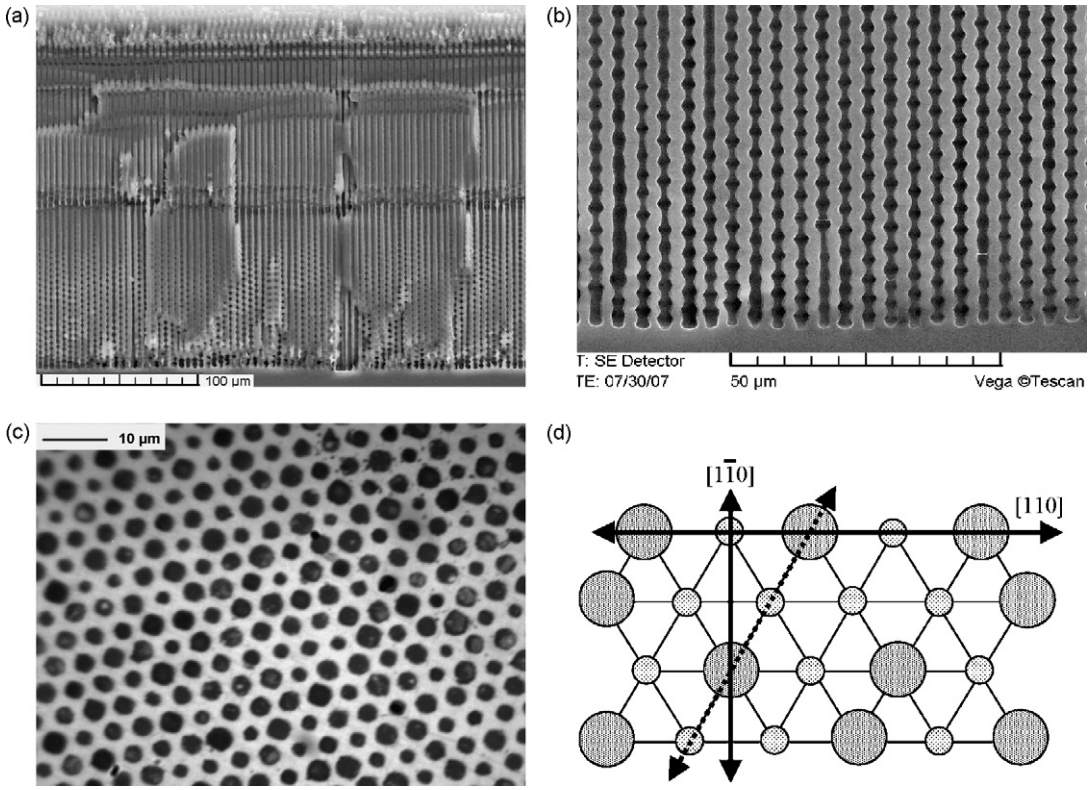

Fig. 8. Self-induced anti-phase pore diameter oscillations in n-type Si. (a) Overview; rather deep pores in n-type Si. (b) Detail of the anti-phase diameter oscillations at large depths. (c) Top view of a plane at the depth of the oscillations. (d) The illustration shows why in a hexagonal lattice a perfect anti-correlation is impossible. A frustrated structure thus results.

pling between neighboring pores, the external current will have a well-defined average and the corresponding voltage is constant. If phase coupling occurs, an external current oscillation should occur, which is not possible under galvanostatic conditions. Instead, the galvanostat adjusts the voltage to keep the current constant and this leads straight to voltage oscillations, cf. [7] for details.

Note, however, that oscillations in space of some pore geometry parameter, and oscillations in time of the current or voltage, are not necessarily always appearing together. In Ge [23], for example, strong voltage oscillations during pore growth did not influence the pore geometry in any obvious or significant way; similar observations were reported for InP [8,9] and recently even for Al_2O_3 [58]. Note also that at least some of the oscillations reported in this context might "simply" be due to conditions where a net growth of SiO_2 is observed, which then flakes off "mechanically" in a periodic manner; e.g. [59–62].

In the examples given for correlated self-induced pore diameter modulations all pores were "in phase", i.e. all pores increased or decreased their diameters at the same time and depth. Rather recently, Cojocaru et al. described self-induced anti-phase oscillations of pores in n-type Si [52,63]; Fig. 8 shows examples. The nucleation of the pores in this case was determined by lithography, the structure was a hexagonal pattern on a {1 0 0} substrate. In hundreds of previous pore etching experiments using the standard pore growth mode (lightly doped {1 0 0} n-type Si, aqueous electrolyte with at most 5 wt% HF, intense back side illumination, lithographically defined nucleation; cf. [1,21]) this kind of behavior was never observed. The novelty in the experiment shown in Fig. 8 was a higher HF concentration with a concomitant higher current, and the addition of "stabilizers" to the electrolyte [52,63].

It is of interest to note that these anti-phase oscillations represent once more a frustrated structure. Fig. 8d demonstrates why in a hexagonal lattice a perfect anti-correlation is impossible. While it is possible to have a large/small sequence of pore diameters in any one direction, this is not possible for all directions in a hexagonal environment. Fig. 8c, showing a top view of pores at the depth of these oscillations, reveals a rather random looking pore diameter distribution. A prediction thus would be that these anti-phase oscillations would be much more pronounced for a square lattice of the nucleation points where no frustration needs to occur.

While the Kiel group indulged in some speculations about the phenomena described above, we will not go deeply into this here, except for pointing out a few first general conclusions.

i) If pore diameter oscillations are encountered, logic dictates that either the current or the current density (or both) must also oscillate. For example, if as postulated for the "standard" n-Si (macro)pores in the so-called "Lehmann model" [1,64], the current density at the pore tip is always constant, the current must oscillate to accommodate the changing dimensions. Since the pores shown in Fig. 8 were obtained at galvanostatic conditions, the current cannot oscillate and we are forced to conclude that in this case the current density oscillates.
ii) Correlated pore diameter oscillations express simultaneously both an intrinsic time constant τ_i and an intrinsic length scale λ_i. It can be reasoned that one follows from the other under certain circumstances or that this kind of self-organization happens as soon as the two numbers happen to "match" in the sense that $\tau_I \cdot \lambda_I = c$ = some special velocity.
iii) In view of this, the several kinds of pore diameter oscillations in several semiconductors provide strong evidence for the point of view that pore etching generally (but not necessarily always) results from a non-linear dynamic system that has not only intrinsic length scales (like the width of the space charge region), but also intrinsic time scales with one or more time

constants τ that go beyond simple relations of the type $\tau = L^2/D$, with L = some intrinsic (diffusion) length [65].

iv) Despite major differences in the (electro)chemistry of various semiconductors, pore etching, if occurring at all, shows some features indicating that there are some underlying principles and mechanisms that transcend the chemical dissolution mechanisms. This point will find even more support in what follows. While the CBM in a generalized form (cf. [46,66]) could provide the necessary "underlying principle" and the intrinsic time constants, there is no direct proof of its validity yet.

If one subscribes to this general point of view, an immediate consequence would be that attempts of modulating pore diameters by modulating an external quantity, usually the current, would be bound to produce "strange" results as soon as the externally enforced time constant $\tau_{ex} = 1/\nu$; ν = frequency of the external modulation signal, interferes with internal ones. This is indeed the case—it has been found that it is rather difficult to produce pore diameter modulations following the externally applied modulation. The Halle group has excelled in overcoming the problems [67], but it should be noted that well-behaved macropore etching systems in this respect are limited to a small part of parameter space for lightly doped n-type Si in aqueous electrolytes (and to all Si mesopore etchings; but that is beyond the scope of this paper), while for other semiconductors, or other conditions, rather strange behavior is usually observed (and rarely published). To give just two examples: etching n-type Si under "standard" conditions but with "organic" electrolytes (i.e. dissolving the HF not in water but in organic solvents) gives rise to strange effects including some kind of "resonance phenomena" [68], while macropores being etched in p-type Si (cf. [69,70] from the leading Michigan group around Bergstrom) usually do not respond at all to current modulations—these pores do not change their diameter but their growth speed if the current is modulated.

A relatively new phenomenon in the context of pore diameter oscillations are "pore bundle" diameter oscillations or pore direc-

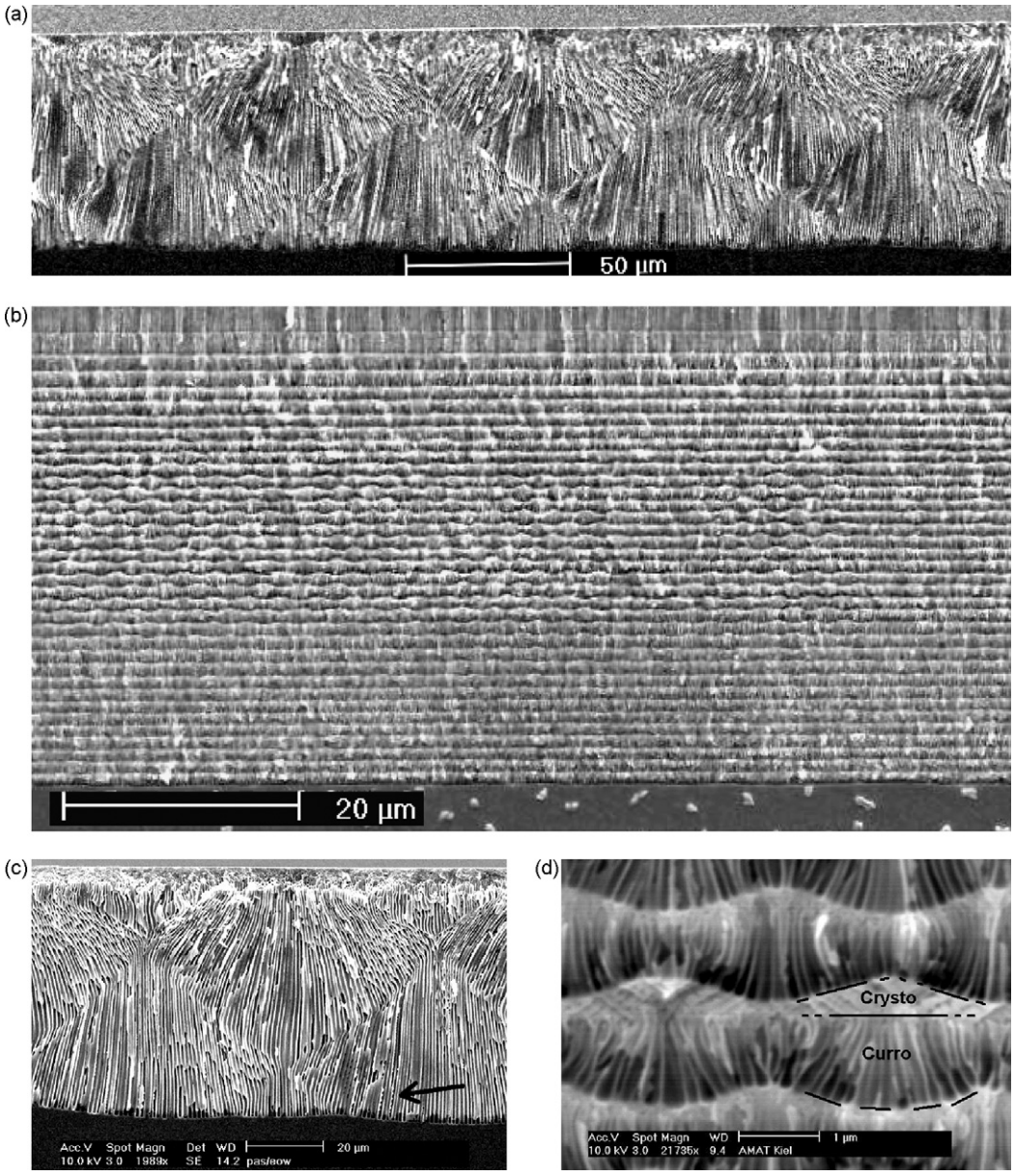

Fig. 9. Self-induced pore-bundle diameter oscillations. (a) Curro pores in {1 0 0} n-type InP; wavelength ≈80 μm. (b) Externally induced periodic switch between crysto and curro pores with self-induced pore bundle oscillations in parts of the depth; wavelength ≈2 μm. (c) Detail of (a). Note that individual pores still show some uncorrelated diameter oscillations; the arrow points to particularly well expressed ones. (d) Detail of (b).

tion oscillations, so far only found in n-type InP, as illustrated in Fig. 9.

The two examples given are the only fully expressed pore bundle oscillations known at present. However, with hindsight, weak and damped pore bundle diameter oscillations could be seen in many old micrographs. Once more, it is necessary to realize that the structure must be either perfectly hexagonal if viewed from above, frustrated, or one-dimensional on the surface, for the reasons already given. Experimentally, it appears that some kind of domain with one-dimensional structure is formed (i.e. the cross-sections shown in Fig. 9 would look the same above or below the cleavage plane shown). A puzzle of sorts is the very long wavelength of around 80 μm observed in one instance (where a highly viscous electrolyte was used [71]), since it does not scale with any intrinsic length scale of the system that might have some bearing on the phenomenon. A speculative explanation, backed by the observations that the electrolyte flow conditions severely influence this kind of oscillation, might be the interaction of the electrolyte flow direction with crystallographic directions. That a pore bundle oscillation if started for whatever reason might continue for some time can be understood in principle within the general model for crysto–curro pore formation championed in [22].

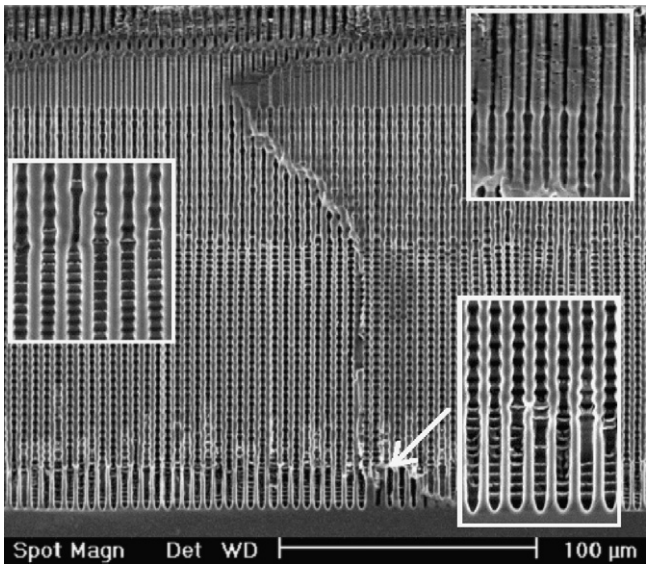

Fig. 10. Macropores in n-type Si growing with a 50% modulation of the current starting at a depth of about 25 μm. The insets illustrate the three growth mode changes encountered.

5. Growth mode transitions

The concept of pore growth mode transition has been introduced fairly recently by the Kiel group, triggered by several new (and unexpected) findings in the context of a "fast etching" variant of the standard n-type Si macropore etching technique already mentioned above. For more than 18 years the etching for deep (depth > 300 μm) Si-n-macro(aqu, bsi) pores was only possible with relatively small current densities in aqueous electrolytes with at most 5 wt% HF. Adding carboxylic acids like acetic acid and/or salts like carboxymethylcellulose sodium salt to the electrolyte not only allowed for far deeper and far "better" pores etched at relatively high HF concentrations and therefore high speed, but also produced a number of very pronounced changes on the pore growth mode, usually with a sudden self-induced growth mode transition. Some examples have already been given; Fig. 5c shows a transition from ⟨1 1 3⟩ oriented crysto pores to possible curro pores (the exact nature is not yet clear) obtained with a 15 wt% HF electrolyte (HF dissolved in a 2:1 H_2O:propionic acid solvent) and relatively high current densities.

The growth mode transition from straight pores to pores exhibiting anti-phase diameter oscillations as shown in Fig. 8 also belongs into this category. Fig. 10 gives another example that also illustrates nicely what has been said about attempting pore diameter modulations by external means in the preceding chapter. In this case a "fast pore growth mode" experiment along the lines given above has been conducted in n-type Si at conditions that would give fairly good and deep pores, but with the current switched periodically at 2 min intervals between the nominal current for that type of experiment and 50% of that value. The result is shown in Fig. 10. The experiment was thus of the "pore diameter modulations by external means" type, and the Lehmann model [1,64] would predict that the pore diameter would follow the current. The experiment proves otherwise. Upon the first reduction of the current, the pore diameters actually seem to increase, as clearly visible in the corresponding inset of Fig. 10. Equally unexpected are two obvious growth mode changes occurring about halfway down the pores and before the last 20 μm or so; both are illustrated by insets.

Again, while there is plenty of room for speculations about the mechanism behind these transitions, we will not indulge at this point, but only point out once more that there is no steady state for at least part of the growing pores.

More details about growth mode transitions in general, including the crysto–curro growth mode transition in Si, InP and GaP, can be found in [52]. A general feature seems to be that these transitions can occur self-induced or might be triggered externally. If they are self-induced, it is a safe bet that the system before the transition is not in some kind of (slowly and smoothly changing) "steady state", but that internal quantities change more rapidly. For example, in the case of the self-induced crysto–curro transition in InP, it is clear that the initial current density after the nucleation of the first crysto pores is too large, inducing the pores to branch repeatedly, quickly decreasing the current density by increasing the active area. This process has been recently modeled in some detail by the Kiel group; first results are represented in the following section.

We may thus state that a growth mode transition is a major change of the system state that occurs if a smoothly changing parameter exceeds some critical value. This is a general feature of non-linear "chaotic" systems and once more supports the point of view that the electrochemistry of semiconductors, including the large part in parameter space that leads to the formation of pores, shares many features with dynamic non-linear systems like self-organization, order–disorder transitions, pattern formation, etc., and that this behavior results to a large extent from some general principles and not so much from the detailed chemistry of the dissolution process.

6. Crysto pores in InP—a case study including a new expression of self-organization

A detailed experimental study of the formation of crysto pores in {1 0 0} n-type InP by Leisner et al. [72] produced the pore density vs. pore depth graph shown in Fig. 11, with the total etching time as parameter. There is a clearly visible "oscillation" of the pore density with pore depth. A three-dimensional Monte Carlo model as illustrated in Fig. 11c with about 1 billion voxels reproduced the experimental findings for a reasonable set of assumptions and parameters, including the pore density oscillations; for details cf. [72] and forthcoming publications. Three assumptions have been made: (i) the valence of the dissolution process is constant, (ii) the branching probability of a pore is proportional to the current density j_{tip} at the pore tip (with different probabilities for branching

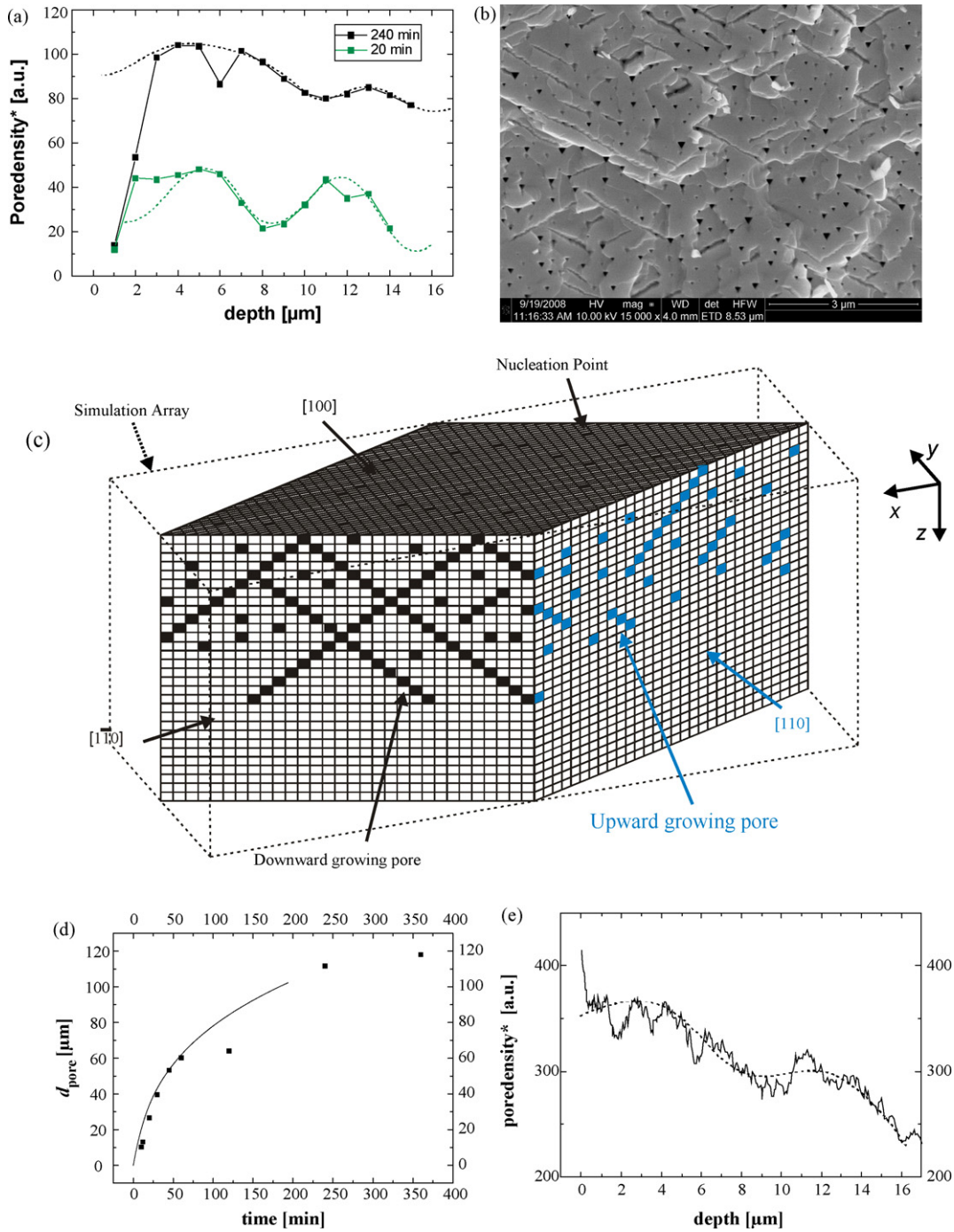

Fig. 11. Crysto pores in InP. (a) Pore density as a function of depth for two different etching times. Wavy lines are to guide the eye and show clear pore density oscillations. (b) Cross-sectional picture of the pores. Downward growing pores are inclined to the cleavage plane and show up as dark triangles; upwardly growing pores are in the cleavage plane and appear as lines. (c) Illustration of the three-dimensional grid used for the Monte Carlo simulation with some model pores drawn in. (d) Simulation results for pore depth as a function of time and experimental data. (e) Simulation results for the pore density as a function of pore depth; compare to (a).

at pore tips and from pore walls), and (iii) pore growth stops if the pore tip approaches a pore wall of another pore.

In a more analytical approach based on the same assumptions a simple equation for the pore depth vs. time could be derived that fits the data rather well. While the CBM was not invoked directly, it is clear that the general stochastic behavior proposed for the pore branching is compatible with the CBM.

It is of interest to note that with hindsight it became clear that oscillatory behavior of the pore density in InP has been observed but not noticed already in [73]. It is also noteworthy to point out that in the InP work reported here, in situ FFT impedance spectroscopy has been used for the first time in the context of crysto pore growth in InP yielding a wealth of results not yet fully evaluated but partially published in [72].

The Monte Carlo simulation could reproduce a number of measured parameters rather well (cf. Fig. 11d), but only shows some indication of pore density oscillations. The difference between measured and simulated data in this case can be easily understood by the limitations of the model, nevertheless the reason for these oscillations becomes clear. They are directly tied to the pore nucleation; the initial nucleation density determines the wavelength of the oscillations. The pore density oscillates after first pores have been

nucleated and started to grow because pore growth and branching is terminated in those areas of the sample where a critical density of pores is reached. This critical density is reached as soon as the space between pores is completely "filled" by space charge regions surrounding the pores. Further pore growth and branching is then impossible or at least slowed down, and pore tips in these areas may be considered "electrically dead". This phenomenon occurs first at regions close to the surface. Since the global current is kept constant, a decreasing number of active pore tips leads to an increase of the current density at these pore tips, enhancing branching and thus also the pore density with depth. In total, the termination of pore growth in the electrically dead layers at a certain depth will increase the pore density in lower regions, resulting in pore density oscillations with depth. The wavelength of these oscillations depends on the nucleation density of the first pore tips, i.e. the mean distance between initial nuclei.

7. In situ measurements

It has become clear by now that pore growth in semiconductors contains some specific, and quite general instances of self-organization, and that a general understanding needs to transcend purely chemical reaction equations. Besides the CBM, no general principle has been proposed so far, and the CBM in its present form is far too simple and limited to carry much further. A severe problem for understanding and modeling the phenomena described is the lack of data. As far as in situ data are concerned, all the experiments reported provide at best the time development of the few extrinsic parameters like current and voltage. As far as microscopic or local data are concerned, the only sources for those are the ex situ microscope pictures provided by cutting the sample. Considering that the tip of the growing pore is the place where most (but not all) of the interesting processes take place, it becomes clear that providing in situ microscopic measurements is exceedingly difficult if not impossible—how does one "look down" some 100 μm at the tip of a growing 1 μm diameter pore?

The Kiel group has endeavored for a long time to do what is possible: in situ multi-mode FFT impedance spectroscopy (IS), and finally succeeded by developing dedicated hard- and software. Details and examples are given in [74]. A fast Fourier transform technique (FFT) is needed in order to obtain complete impedance spectra in a time short enough for meaningful in situ data; "multi-mode" refers to the option to modulate the illumination intensity whenever applicable in addition to the (conventional) current or voltage.

Raw impedances spectra are of limited use, however, and detailed models for the theoretical impedance had to be developed. In some cases like the standard n-Si-macro(aqu, bsi) etching, modeling has progressed far enough to allow the in situ extraction of quantitative primary data like the pore depth or the valence of the dissolution process [74]. In the case of InP, pronounced dif-

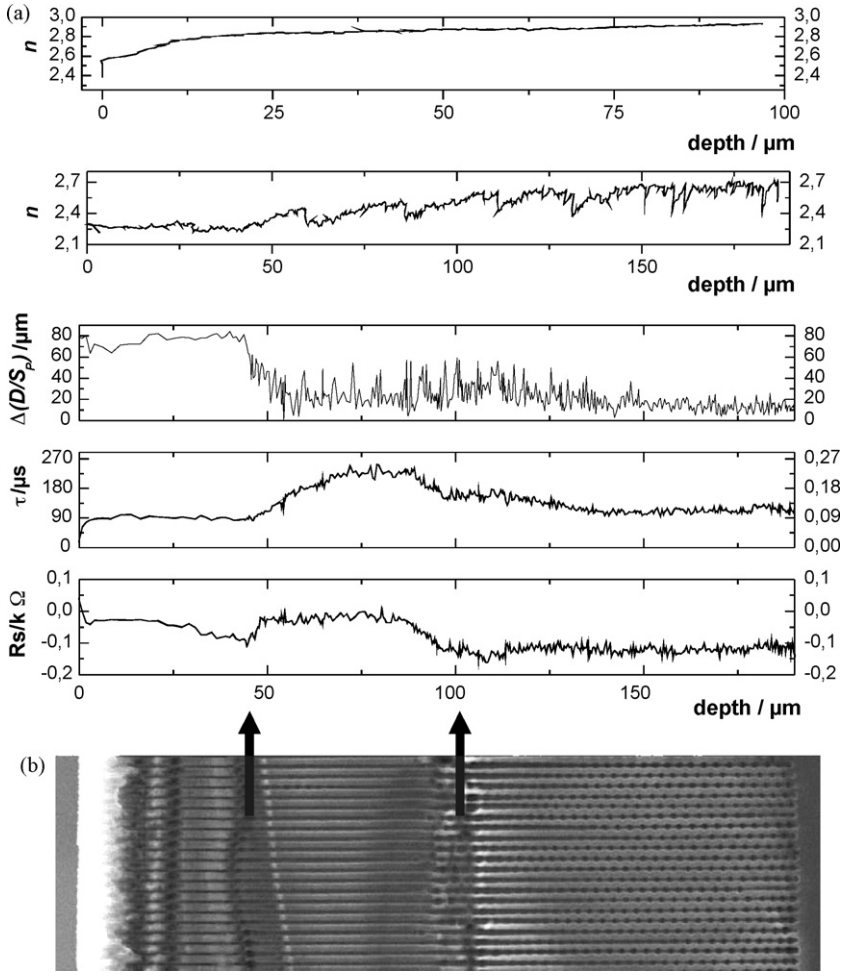

Fig. 12. Examples of in situ data obtained during pore etching experiments of n-type silicon macropores. The data were converted from a function of time to functions of depth using the in situ measured pore depth values. (a) Valence for two experiments yielding almost identical pore geometries. (b) Development of 3 parameters as a function of pore depth for the pores shown, exhibiting two pronounced growth mode transitions. For details see text.

ferences in the etching process kinetics for crysto and curro pores have been found [71] but models beyond some suitable equivalent-circuit descriptions [72,75] have yet to be developed; the approach described above is one step in this direction.

While IS cannot give local microscopic information, it can provide in situ average information. The application of two-mode in situ FFT IS to the n-Si-macro(aqu, bsi) pore growth yields not only about 10 in situ parameters – besides the quantities mentioned, for example also the size of the advancing etch front (i.e. the degree of under etching) – but also evidence that a growing pore tip cannot process the incoming holes all the time and is most likely covered with oxide most of the time [74]. Moreover, IS allows to "watch" growth mode transitions as they happen. Fig. 12 shows a few illustrative results.

Fig. 12a essentially demonstrates the difference between a standard 5 wt% HF electrolyte (upper curve) and a viscous 10 wt% electrolyte (lower curve) used for etching Si-n-macro(aqu, bsi) pores. In the second case (lower curve) the pore depth was accordingly larger for about the same etching time while the geometry and quality of the pores was rather similar. Most remarkable is the observation that the valence of the process (required to be about 2.7 for "good" pores) shows a very unruly behavior for the viscous electrolyte that might indicate (failed) attempts of the system to initiate a growth mode transition in steps of roughly 25 μm. The data are insufficient for a time sequence analysis but might be tentatively interpreted as an indication of "chaotic" behavior. The fluctuations shown are not visible in the pore shape, i.e. in a "post-mortem" analysis.

Fig. 12b shows an example with the growth mode transition to the anti-phase diameter oscillations described in Section 4, occurring at a depth of about 100 μm. There is, however, another mode transition (aborted cavity formation) at a depth of about 40 μm, indicated by an arrow. The three parameters shown are the "hole processing power" $\Delta(D/S_p)$ of the pore tip expressed quantitatively by the difference of a recombination velocity S (in combination with the diffusion coefficient D of the holes), a time constant τ tied to the kinetics of the oxide dissolution process, and the total (differential) serial resistance R_s of the system. All three parameters respond markedly to the two growth mode transitions observed and provide quantitative input for modeling what is actually happening. Some first tentative evaluation of these and other data can be found in [63].

8. Discussion

It has been shown that anodic dissolution of semiconductors provides for a large number of self-organization features in time and space—some rather spectacular like the self-organized formation of three-dimensional pore crystals in InP or the anti-phase diameter oscillations of macropores in Si, some rather hidden like the ones indirectly showing up in the second curve of Fig. 12a. It has also been shown that there is a number of features common to several semiconductors and that there must be intrinsic time and length scales that are expressed in the observed spatial and temporal pattern formations. While there are many lateral length scales found for pore etching in semiconductors, spanning the range from radii of curvature of pore tips tied to electrical breakdown, dimension of the space charge region, the minority carrier diffusion length, or scales emerging from a stability analysis of the advancing interface [20,21,76], not much has been reported with respect to length scales into the depth of the pore or the time scales.

This is not to say that there is no understanding at all of what happens during pore etching as a function of depth. It is clear, for example, that the current flowing through the pore walls, inducing lateral pore growth and eventually cavity formation, increases with pore depth until it reaches a critical magnitude in relation to the external current. While the pore wall current density is far smaller than the pore tip current density (and a function of the degree of pore wall passivation), the current simply increases linearly with the pore length. In a similar vein, the diffusion (and drift) of molecules and ions in and out of the pore will always introduce length and time scales that are related to the pore depth, cf. [65] and the references therein for a recent effort in this direction. In contrast to the impedance spectroscopy results, however, these scales tend to change smoothly as a function of depth and it is fair to state that none of the insights alluded to above includes the self-organization and pattern formation topics addressed here in any direct or indirect way.

Looking at just pore growth in Si, several particle currents need to flow into and out of the pore to provide or remove molecules and ions from the advancing front and to carry the electrical current. While the supply of neutral HF to the pore tip would have to depend exclusively on diffusion current and thus gradients in the concentration, the ions carrying the (constant) electrical current must experience some drift or field component since it is impossible to do this exclusively with diffusion currents over the whole depth range. One might speculate that growth mode transitions can be tied to a kind of switch over from predominantly diffusion currents at smaller pore depths to predominantly field currents at larger depths, and that this can happen during pore growth in other semiconductors, too, but it is premature at present to enlarge upon this topic. The number of experiments yielding some self-organization feature in semiconductor electrochemistry has grown substantially in recent years and it can be expected that this trend will continue for some time. While it is clear that just one general model will not be able to account for all the self-organization phenomena presented here (or for the ones found in the future), it is equally clear that not every experimental observation needs its own model either. There is definitely some common ground, e.g. in the crysto–curro transition observed in several systems by now.

9. Conclusions

This paper has been a first attempt in sorting through the self-organization phenomena encountered in semiconductor electrochemistry so far. At present, the enumeration of the effects found still takes precedence over a coherent ordering of phenomena within some established theoretical framework. The current burst model outlined here in a cursory way, in the opinion of the authors, will be part of that framework in some version. Not only does it introduce an intrinsic time scale that, in its generalized form, may have some bearing on the problem posed, it also contains a stochastic component that at least in the case of the current and voltage oscillation of a Si electrode, allows both complete randomness with respect to pattern formation and complete order, with order–disorder transitions occurring as a function of the system parameters.

Acknowledgements

The authors are indebted to Prof. K. Krischer who encouraged us to do this kind of survey, and to Profs. J.-N. Chazalviel, F. Ozanam, G. Popkirov, and J. Grzanna for many discussions and helpful comments.

References

[1] V. Lehmann, Electrochemistry of Silicon, Wiley–VCH, Weinheim, 2002.
[2] E. Foca, J. Carstensen, G. Popkirov, H. Föll, ECS Trans. 6 (2) (2007) 345.

[3] J.-N. Chazalviel, F. Ozanam, M. Etman, F. Paolucci, L.M. Peter, J. Stumper, J. Electroanal. Chem. 327 (1992) 343.
[4] J. Grzanna, H. Jungblut, H.J. Lewerenz, J. Electroanal. Chem. 486 (2000) 190.
[5] K. Krischer, H. Varela, in: W. Vielstich, A. Lamm, H. Gasteiger (Eds.), Handbook of Fuel Cells, vol. 2 (6), John Wiley & Sons, Ltd., 2003, p. 679.
[6] E. Foca, J. Carstensen, H. Föll, J. Electroanal. Chem. 603 (2007) 175.
[7] S. Langa, J. Carstensen, I.M. Tiginyanu, M. Christophersen, H. Föll, Electrochem. Solid-State Lett. 4 (6) (2001) G50.
[8] E. Harvey, D.N. Buckley, S.N.G. Chu, Electrochem. Solid-State Lett. 5 (4) (2002) G22.
[9] C. O'Dwyer, D.N. Buckley, S.B. Newcomb, J. Electrochem. Soc. 21 (18) (2005) 8090.
[10] A.M. Gonçalves, L. Santinacci, A. Eb, I. Gerard, C. Mathieu, A. Etcheberry, Electrochem. Solid-State Lett. 10 (4) (2007) D35.
[11] Y.H. Ogata, T. Itoh, M.L. Chourou, K. Fukami, T. Sakka, ECS Trans. 16 (3) (2008) 181.
[12] K. Krischer, Nonlinear dynamics in electrochemical systems, volume 8, in: R.C. Alkire, D.M. Kolb (Eds.), Advances in Electrochemical Science and Engineering, vol. 89, Wiley–VCH, Weinheim, 2003.
[13] J.-N. Chazalviel, F. Ozanam, ECS Trans. 16 (3) (2008) 189.
[14] S. Langa, I.M. Tiginyanu, J. Carstensen, M. Christophersen, H. Föll, Appl. Phys. Lett. 82 (2) (2003) 278.
[15] X.G. Zhang, Electrochemistry of Silicon and its Oxide, Kluwer Academic–Plenum Publishers, New York, 2001.
[16] R.L. Smith, S.D. Collins, J. Appl. Phys. 71 (8) (1992) R1.
[17] O. Bisi, S. Ossicini, L. Pavesi, Surf. Sci. Rep. 38 (2000) 1.
[18] S. Ossicini, L. Pavesi, F. Priolo, Light Emitting Silicon for Microphotonics, Springer, Berlin, 2003.
[19] V. Lehmann, S. Stengl, A. Luigart, Mater. Sci. Eng. B 69–70 (2000) 11.
[20] J.-N. Chazalviel, R. Wehrspohn, F. Ozanam, Mater. Sci. Eng. B 69–70 (2000) 1.
[21] H. Föll, M. Christophersen, J. Carstensen, G. Hasse, Mater. Sci. Eng. R 39 (4) (2002) 93.
[22] H. Föll, S. Langa, J. Carstensen, S. Lölkes, M. Christophersen, I.M. Tiginyanu, Adv. Mater. 15 (3) (2003) 183.
[23] C. Fang, H. Föll, J. Carstensen, J. Electroanal. Chem. 589 (2006) 259.
[24] M. Faraday, Phil. Trans. R. Soc., Ser. A 124 (1834) 77.
[25] O. Teschke, F. Galambeck, M.A. Tenan, J. Electrochem. Soc. 132 (6) (1985) 1284.
[26] P. Russell, J. Newman, J. Electrochem. Soc. 133 (1) (1986) 59.
[27] P. Russell, J. Newman, J. Electrochem. Soc. 134 (5) (1987) 1051.
[28] W. Wang, I.Z. Kiss, J.L. Hudson, Chaos 10 (1) (2000) 248.
[29] Z. Fei, R.G. Kelly, J.L. Hudson, J. Phys. Chem. 100 (49) (1996) 18986.
[30] A.J. Pearlstein, H.P. Lee, K. Nobe, J. Electrochem. Soc. 132 (9) (1985) 2159.
[31] M.R. Bassett, J.L. Hudson, J. Electrochem. Soc. 137 (3) (1990) 922.
[32] M.R. Bassett, J.L. Hudson, J. Electrochem. Soc. 137 (6) (1990) 1815.
[33] W. Li, X. Wang, K. Nobe, J. Electrochem. Soc. 137 (4) (1990) 1184.
[34] U.F. Franck, Angew. Chem. 90 (1978) 1.
[35] W. Jessen, Naturwissenschaften 65 (9) (1978) 449.
[36] U.F. Franck, Ber. Bunsenges. Phys. Chem. 84 (1980) 334.
[37] J. Carstensen, R. Prange, G.S. Popkirov, H. Föll, Appl. Phys. A 67 (4) (1998) 459.
[38] J. Carstensen, R. Prange, H. Föll, J. Electrochem. Soc. 146 (3) (1999) 1134.
[39] J. Grzanna, H. Jungblut, H.J. Lewerenz, J. Electroanal. Chem. 486 (2000) 181.
[40] J. Grzanna, H. Jungblut, H.J. Lewerenz, Phys. Stat. Sol. (a) 204 (5) (2007) 1245.
[41] W. Wolf, M. Lübke, M.T.M. Koper, K. Krischer, M. Eiswirth, G. Ertl, J. Electroanal. Chem. 339 (1995) 185.
[42] K. Krischer, J. Electroanal. Chem. 501 (2001) 1.
[43] J.-N. Chazalviel, F. Ozanam, J. Electrochem. Soc. 139 (9) (1992) 2501.
[44] F. Ozanam, N. Blanchard, J.-N. Chazalviel, Electrochim. Acta 38 (12) (1993) 1627.
[45] J. Grzanna, T. Notz, H.J. Lewerenz, ECS Trans. 16 (3) (2008) 173.
[46] J. Carstensen, M. Christophersen, H. Föll, Mater. Sci. Eng. B 69–70 (2000) 23.
[47] O. Jessensky, F. Müller, U. Gösele, J. Electrochem. Soc. 145 (11) (1998) 3735.
[48] J.M. Macak, H. Hildebrand, U. Marten-Jahns, P. Schmuki, J. Electroanal. Chem. 621 (2008) 254.
[49] S. Berger, J. Faltenbacher, S. Bauer, P. Schmuki, Phys. Stat. Sol. RRL 2 (3) (2008) 102.
[50] S. Frey, M. Kemell, J. Carstensen, S. Langa, H. Föll, Phys. Stat. Sol. (a) 202 (8) (2005) 1369.
[51] S. Langa, J. Carstensen, M. Christophersen, K. Steen, S. Frey, I.M. Tiginyanu, H. Föll, J. Electrochem. Soc. 152 (8) (2005) C525.
[52] A. Cojocaru, J. Carstensen, H. Föll, ECS Trans. 16 (3) (2008) 157.
[53] G. Toulouse, Commun. Phys. 2 (4) (1977) 115.
[54] P.W. Anderson, Phys. Rev. 102 (4) (1956) 1008.
[55] P.P. Crooker, Liq. Cryst. 5 (3) (1989) 751.
[56] M. Christophersen, S. Langa, J. Carstensen, I.M. Tiginyanu, H. Föll, Phys. Stat. Sol. (a) 197 (1) (2003) 197.
[57] S. Langa, J. Carstensen, I.M. Tiginyanu, M. Christophersen, H. Föll, Electrochem. Solid-State Lett. 5 (2002) C14.
[58] K. Schwirm, W. Lee, R. Hillebrand, M. Steinhart, K. Nielsch, U. Gösele, ACS Nano 2 (2) (2008) 302.
[59] V.P. Parkhutik, Electrochim. Acta 36 (10) (1991) 1611.
[60] V. Parkhutik, Solid State Electron. 45 (2001) 1451.
[61] V. Lehmann, J. Electrochem. Soc. 143 (4) (1996) 1313.
[62] M. Leisner, J. Carstensen, H. Föll, J. Electroanal. Chem. 615 (2) (2008) 124.
[63] A. Cojocaru, J. Carstensen, M. Leisner, H. Föll, I.M. Tiginyanu, Phys. Stat. Sol. (c), in press.
[64] V. Lehmann, J. Electrochem. Soc. 140 (10) (1993) 2836.
[65] G. Barillaro, F. Pieri, J. Appl. Phys. 97 (2005) 116105.
[66] J. Carstensen, M. Christophersen, G. Hasse, H. Föll, Phys. Stat. Sol. (a) 182 (1) (2000) 63.
[67] S. Matthias, F. Müller, J. Schilling, U. Gösele, Appl. Phys. A 80 (7) (2005) 1391.
[68] H. Föll, J. Carstensen, M. Christophersen, G. Hasse, Phys. Stat. Sol. (a) 182 (1) (2000) 7.
[69] J. Zheng, M. Christophersen, P.L. Bergstrom, Phys. Stat. Sol. (a) 202 (8) (2005) 1402.
[70] J. Zheng, M. Christophersen, P.L. Bergstrom, Phys. Stat. Sol. (a) 202 (8) (2005) 1662.
[71] H. Föll, J. Carstensen, E. Foca, M. Leisner, ECS Trans. 6 (2) (2007) 309.
[72] M. Leisner, J. Carstensen, A. Cojocaru, H. Föll, ECS Trans. 16 (3) (2008) 133.
[73] E. Spiecker, M. Rudel, W. Jäger, M. Leisner, H. Föll, Phys. Stat. Sol. (a) 202 (15) (2005) 2950.
[74] J. Carstensen, E. Foca, S. Keipert, H. Föll, M. Leisner, A. Cojocaru, Phys. Stat. Sol. (a) 205 (11) (2008) 2485.
[75] M. Leisner, J. Carstensen, A. Cojocaru, H. Föll, Phys. Stat. Sol. (c), in press.
[76] R.B. Wehrspohn, F. Ozanam, J.-N. Chazalviel, J. Electrochem. Soc. 146 (9) (1999) 3309.